Spectrochimica Acta Part A: Molecular and Biomolecular Spectroscopy 217 (2019) 60–67

Contents lists available at ScienceDirect

Spectrochimica Acta Part A: Molecular and Biomolecular Spectroscopy

journal homepage: www.elsevier.com/locate/saa

Synthesis of nitrogen-doped graphene quantum dots (N-GQDs) from marigold for detection of Fe^{3+} ion and bioimaging

Ying-Peng Zhang [a,*], Ji-Mei Ma [a], Yun-Shang Yang [a,*], Jia-Xi Ru [b], Xiao-Yu Liu [a], Ying Ma [a], Hui-Chen Guo [b]

[a] School of Petrochemical Engineering, Lanzhou University of Technology, Lanzhou 730050, China
[b] State Key Laboratory of Veterinary Etiological Biology and Key Laboratory of Animal Virology of Ministry of Agriculture, Lanzhou Veterinary Research Institute, Chinese Academy of Agricultural Sciences, Lanzhou 730046, China

ARTICLE INFO

Article history:
Received 19 September 2018
Received in revised form 10 March 2019
Accepted 17 March 2019
Available online 19 March 2019

Keywords:
Nitrogen-doped graphene quantum dots
Fe^{3+}
Bioimaging

ABSTRACT

Graphene quantum dots (GQDs) are synthesized by the method of high-temperature pyrolysis from marigold granules and subsequently nitrogen-doped graphene quantum dots (N-GQDs) are synthesized from ethylenediamine by hydrothermal treatment, which shows a strong blue emission with 7.84% quantum yield (QY). This will be used in detection of Fe^{3+} in water environments and the field of bioimaging.

1. Introduction

The development of carbon nanomaterials is rapid, and they are highly sought after by scientists due to their good water solubility, low cytotoxicity, surface modifiability and good electrical conductivity, etc. [1]. There are many such materials as carbon dots (CDs), [2,3] nanodiamonds [4], carbon nanotubes [5], fullerene [6], and fluorescent graphene [7,8]. While carbon dots (CDs) are the collective name for carbon quantum dots (CQDs) and graphene quantum dots (GQDs). Among them, GQDs are a relatively new type of carbon nanomaterials which show interesting fluorescence properties, such as tunable luminous color, excitation wavelength-dependent luminescence, pH-sensitive fluorescence and upconversion luminescence, it has been applied to the field of metal ion detection [9]. There are many materials for synthesizing GQDs, such as graphite powder [10], citric acid [11], SWNTs[b] [12], MWNTs[c] [13] and glucose [14]. However, the synthesis of GQDs from natural biomass is rarely reported. Biomass has a lot of oxygen and carbon fibers, and there are few other elements, which allows biomass to produce high porosity forms of carbon that are called turbine type carbon when pyrolyzed [15,16]. Since marigold has a large amount of lutein we used in this work as a carbon source at 1000 °C annealing would decompose large carbon nuclear into turbostratic carbon and then acidified with strong acid to obtain GQDs with large oxygen functional groups on the surface. These GQDs can be surface-functionalized simply. We doped GQDs with ethylenediamine successfully. Importantly, we have demonstrated that N-GQDs can selectively sense Fe^{3+} ions in water.

High concentration of metal ions in the environment will cause heavy environmental pollution, so it is of great significance to design and develop a kind of fluorescence sensor with rapid, sensitive and selective identification of metal ions [17–19]. Wang et al. first reported that the selective identification of Fe^{3+} by GQDs as fluorescent probed on the basis of the selective turn-off sensing by Fe^{3+} ions [20]. Currently, fluorescence probe based on gold nanoparticles [21] and CDs [22] have been used to detect Fe^{3+} ions. Li et al. reported that the charge transfer quenching was based on the fluorescence of the GQDs in the presence of Hg^{2+} ions and come up with a sensitive detection system of melamine fluorescence [23]. Yu et al. described the assays that GQDs as a fluorescent probe for sulfide ion-sensitive and selective, even at high ion concentrations, strong and stable blue fluorescence can be emitted. Moreover, because of the existence of Cu^{2+}, GQDs aggregation resulted in fluorescence quenching [24].

So far, a large number of methods have come out to improve GQDs productivity [25]. It has been reported that chemical doping with hybrid atoms is an effective way to adjust the intrinsic properties of nanomaterials [26–29]. Due to quantum constraints and edge effects, the electronic properties of GQDs can be fine-tuned by manipulating the chemical and optical properties of N atoms doped with chemical bonds. Several ways of binding nitrogen groups to GQDs framework have been proposed, such as electrochemical treatment and solution chemistry methods [30]. Qu et al. first reported the preparation of N-doped GQDs [31]. Anil et al. reported that a variety of metal ions were added to Am-GQDs solution and many metal ions had a quenching effect on the fluorescence of Am-GQDs, but only the fluorescence of

* Corresponding authors.
E-mail addresses: yingpengzhang@126.com (Y.-P. Zhang), yangyunshang@tom.com (Y.-S. Yang).

https://doi.org/10.1016/j.saa.2019.03.044
1386-1425/

Am-GQDs added Ag^{+} would recover when L-cysteine was added [32]. Hu et al. reported that N-GQDs with a strong blue emission was obtained by hydrothermal treatment of graphene oxide, which was used to image to the biology HeLa cells and showed strong luminescence and excellent biocompatibility [33]. Tam et al. reported that N-GQDs were prepared with carbonization of citric acid by hydrothermal treatment in the presence of ammonia and fluorescent sensors for measuring Fe^{3+} ions have been confirmed [34]. Li et al. prepared the N-O-GQDs with small size, abundant active sites and easy assembly into the electric film by the method of co-doped N and O, which has better performance than lithium battery and can be used as the chip power supply of various micro periods [35].

On account of the discharge of industrial wastewater, the water treatment agent of iron is widely used for water treatment and the content of Fe^{3+} in water gradually increases, which seriously affects the water quality of estuary water and drinking water. The water with high iron content is easy to grow iron bacteria in the pipeline and increasing the turbidity of water, which make water produce special color, smell and taste. It is easy to contaminate clothes, utensils, and affect the quality of some industrial products. When the iron content reaches 0.3 mg/L, the chromaticity is about 20 degrees. At 0.5 mg/L, the chroma can be greater than 30 degrees. At 1.0 mg/L, it can feel the obvious metallic taste, which is unsuitable for cooking and brewing tea. Therefore, it is necessary to develop a low-cost, rapid and sensitive method for the detection of Fe^{3+}.

In this work, we tried to transform the marigold granules after thermal cracking as carbon source into turbostratic carbon and through the further hydrothermal treatments, we succeed in getting the N-GQDs for sensitive and selective detection of Fe^{3+}. The experiment proved that nitrogen-doped GQDs have better photoluminescence properties than undoped GQDs.

2. Experimental Section

2.1. Materials

The biomass used in this experiment, namely marigold granules, which were made by compressing and fermenting natural marigold petals without adding other chemicals were purchased from Gansu Province Sunray Natural Pigment Co., Ltd. (Dry marigold flower can also be used in this work). ethylenediamine, $AgNO_3$, $Al(NO_3)_3$, $Ba(NO_3)_2$, $Ca(NO_3)_2$, $CdCl_2$, $Cu(NO_3)_2$, $Co(NO_3)_2$, $Fe(NO_3)_3$, $Fe(NO_3)_2$, $HgCl_2$, KNO_3, $Mg(NO_3)_2$, $NaNO_3$, $Ni(NO_3)_2$, $Pb(NO_3)_2$, $Zn(NO_3)_2$ were obtained from Sinopharm Chemical Reagent (Shanghai, China) and the concentration of all these metal ions was 10 mM. H_2SO_4 (98%) and HNO_3 (65%) were purchased from Beijing Chemical Factory and used directly without any further purification. All the water used in the experiment was deionized water. PBS solution was configured with Na_2HPO_4, Na_2HPO_4 and NaCl.

2.2. Characterizations

Photoluminescence (PL) spectra were recorded on an LS-55 luminescence spectrometer (Japan). UV–vis absorption spectra were collected on a T6 New Century using a 1 cm path length quartz cell. Raman spectra were taken with a JY-HR 800 micro-Raman with the excitation wavelength at 514 nm. Transmission electron microscopy (TEM) analyses were measured by a JEM-2010 electron microscope (Japan). X-ray photoelectron spectroscopy (XPS) was acquired on the elemental composition of the complex (Thermo Fisher Scientific, UK). X-ray diffraction (XRD) was performed on a Philips X'Pert PRO. Fourier transform infrared (FT-IR) spectra were recorded using an FT-IR-580 spectrophotometer. Fluorescence quantum yield (QY) was collected on the FLs920 steady state/transient fluorescence spectrometer.

2.3. Synthesis of Graphene Quantum Dots

Methods for synthesizing GQDs refer to articles by Anil et al. [32]. The synthetic route is shown in the Fig. 1. Apply an adequate amount of marigold granules dried in an oven at 60 °C, then dry granules ground to get a fine powder. The powder was then pyrolyzed in the tube furnace at 1000 °C for 5 h in Ar atmosphere. Crushed the resulting black powder for 1.5 h to prepare for the synthesis of GQDs. Added 2 g blank power of carbon into the acid mixture of H_2SO_4 and HNO_3 (3:1) and then heated the reflux at 90 °C for 5 h. Subsequently, a large amount of deionized water was added to the solution for filtration with a water filtration membrane of 0.22 μm. The solution contained a large amount of green fluorescent GQDs, which needed to neutralize by NaOH, further dialysis treatments were needed (3500 D, 36 h). Finally, the dialysis solution was dried in the desiccant to get the brown powder, 0.5 g of brown powder was dispersed in 10 mL deionized water and then passed through a 0.22 μm water filtration membrane to obtain a GQDs solution.

2.4. Synthesis of Nitrogen-doped Graphene Quantum Dots

As Fig. 1 shown, the brown powder was dispersed in 20 mL of deionized water and 20 mL of ethylenediamine mixed solution which was transferred to an autoclave for hydrothermal treatment at 200 °C for 10 h. Filtration to remove the excess solution and the product dispersed in 10 mL of deionized water to obtain a highly stable solution of N-GQDs for further testing.

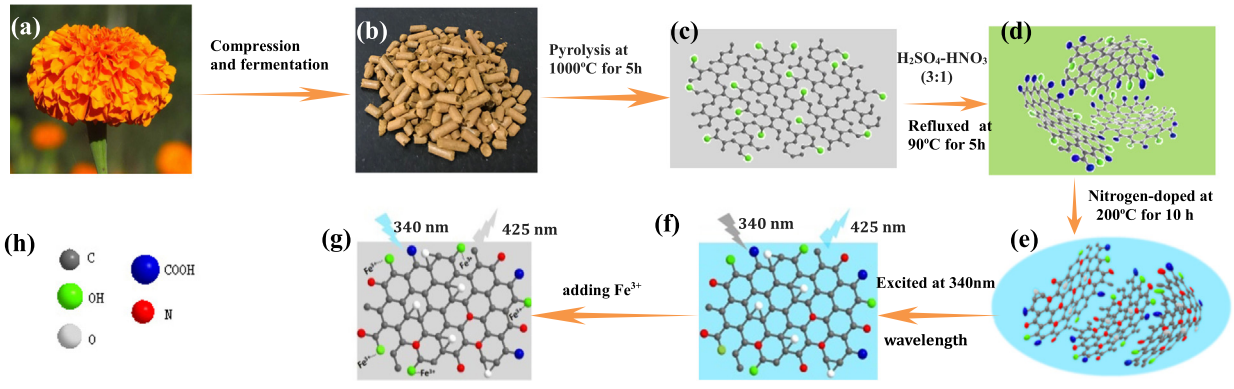

Fig. 1. Synthetic route of N-GQDs and (a) is marigold flower, (b) is marigold granules, (c) is turbostratic carbon, (d) is GQDs, (e) is N-GQDs, (f) is blue fluorescence at 340 nm excitation wavelength, (g) Fluorescence quenching after adding Fe^{3+} and (h) is different atoms.

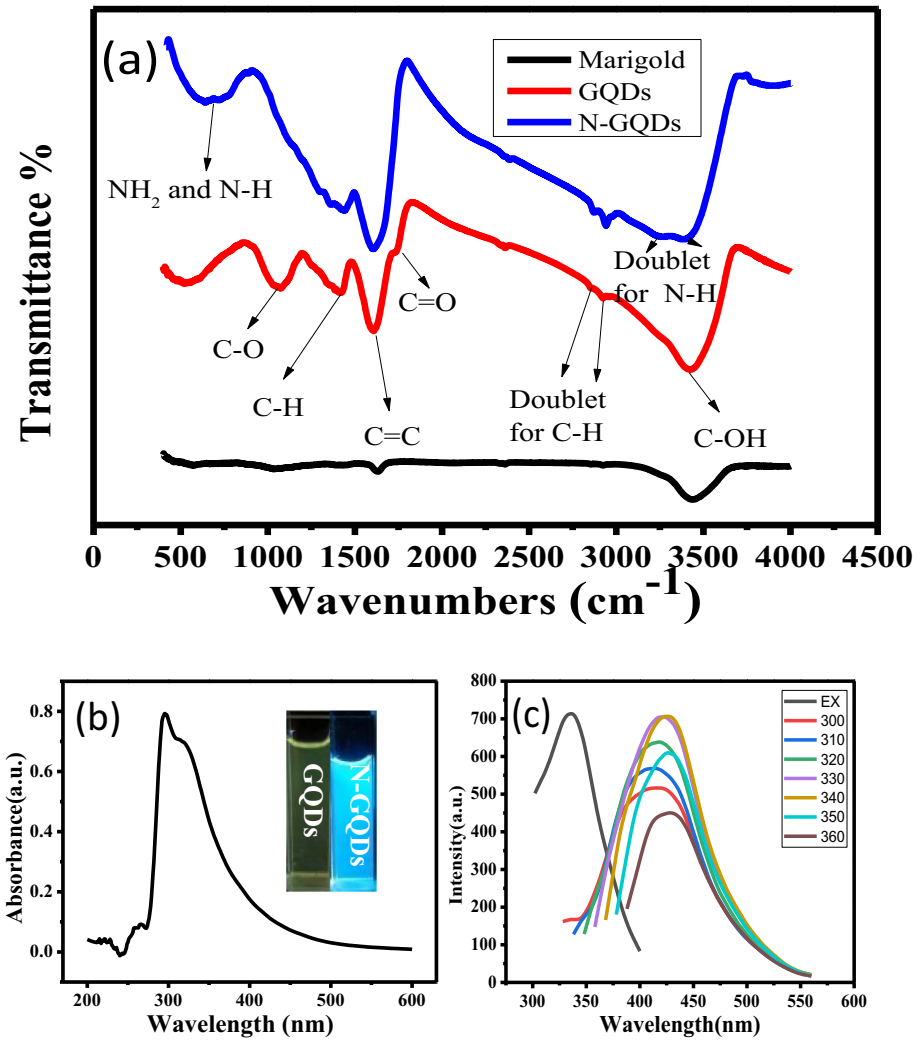

Fig. 2. (a) Is FT-IR spectrum of marigold, GQDs and N-GQDs, (b) is UV–vis absorption spectrum of N-GQDs, the illustration shows the fluorescence of GQDs and N-GQDs under a 365 nm wavelength Uv lamp, and (c) is emission and excitation spectrum of N-GQDs.

2.5. Detections for Fe^{3+} Ions

To measure the fluorescence spectrum of the N-GQDs-Fe (III) system accurately, 10 μL of N-GQDs (18.6 mg/mL) was dissolved in a 100 mL volumetric flask in advance and shaken for immediate use in later experiments. The solution concentration of Fe^{3+} ions and other metal ions need to be configured in advance. The fluorescence spectrum was performed at an excitation wavelength of 340 nm and all slits were 10 nm.

2.6. Detection of Fe^{3+} in the Real Sample

The actual water samples were derived from the Yellow River, which flows through Lanzhou city, Gansu province, China. Centrifugation was

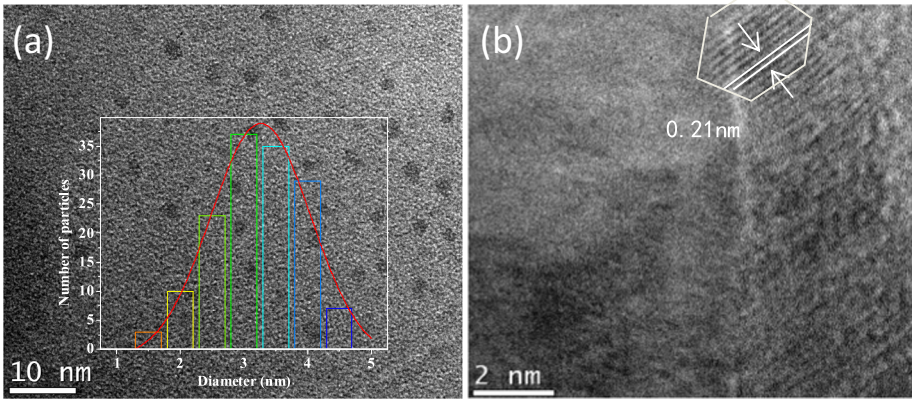

Fig. 3. (a) Is TEM image of N-GQDs, the illustration is the size distribution of N-GQDs, (b) is HRTEM image of N-GQDs.

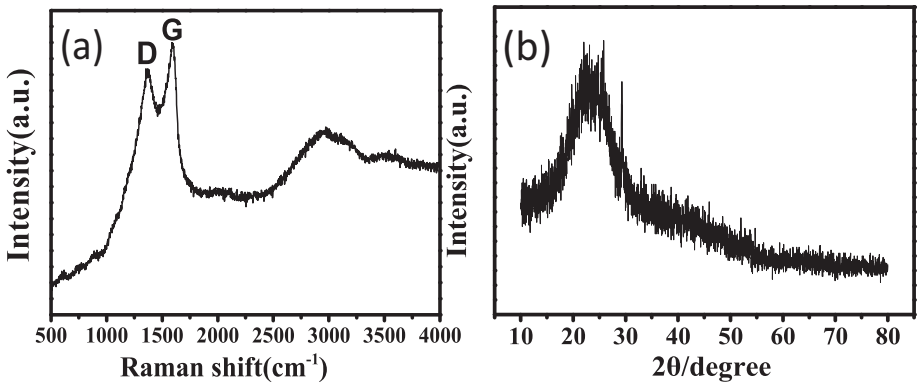

Fig. 4. (a) Is Raman spectrum of N-GQDs, (b) is XRD specture of N-GQDs.

performed at 8000 rpm for 10 min twice to remove a large number of solid impurities in the water, then filtered small particles impurities with filtration membrane whose diameter is 0.22 μm. The treated samples were sealed and stored without adding Fe^{3+}, which were directly used to measure the Fe^{3+} concentration in the water sample.

2.7. Cell Culture and Cellular Imaging Experiment

HeLa cells were provided by the Lanzhou veterinary research institute, Chinese academy of agricultural sciences. HeLa cells were grown in DMEM medium supplemented with 10% embryonic bovine serum and 1% penicillin and streptomycin. Cells (5×10^8 L^{-1}) were placed in 12-well plates at 37 °C in a 5% CO_2 and allowed to adhere for 16 h for cell imaging. N-GQDs (50 μg/mL) was added into cultured HeLa cells for incubation for 4 h. The cells were rinsed with PBS buffer solution for cell imaging experiments. After that, a solution of Fe^{3+} (100 μM) was added into the cell fluid in which the cells are cultured. The next imaging experiment was carried out after incubation for 30 min under the same conditions. Live cell fluorescence imaging was performed using an Olympus IX73 fluorescence microscope.

2.8. Cytotoxicity Test

The toxicity of N-GQDs to HeLa cells was determined by MTS method. HeLa cells in logarithmic growth stage were taken and digested with trypsin. The cells were re-suspended in DMEM medium containing 10% calf serum and seeded to the 96-well plates. Subsequently, cells were cultivated for 24 h at 37 °C in a 5% CO_2 incubator and treated with different concentrations of N-GQDs for another 24 h. MTS (10 μL/hole) were added in the hole and incubated for 3 h. The absorbance at 490 nm was measured with an enzyme-linked immunosorbent assay (ELISA) reader (Bio-Rad, Model 550).

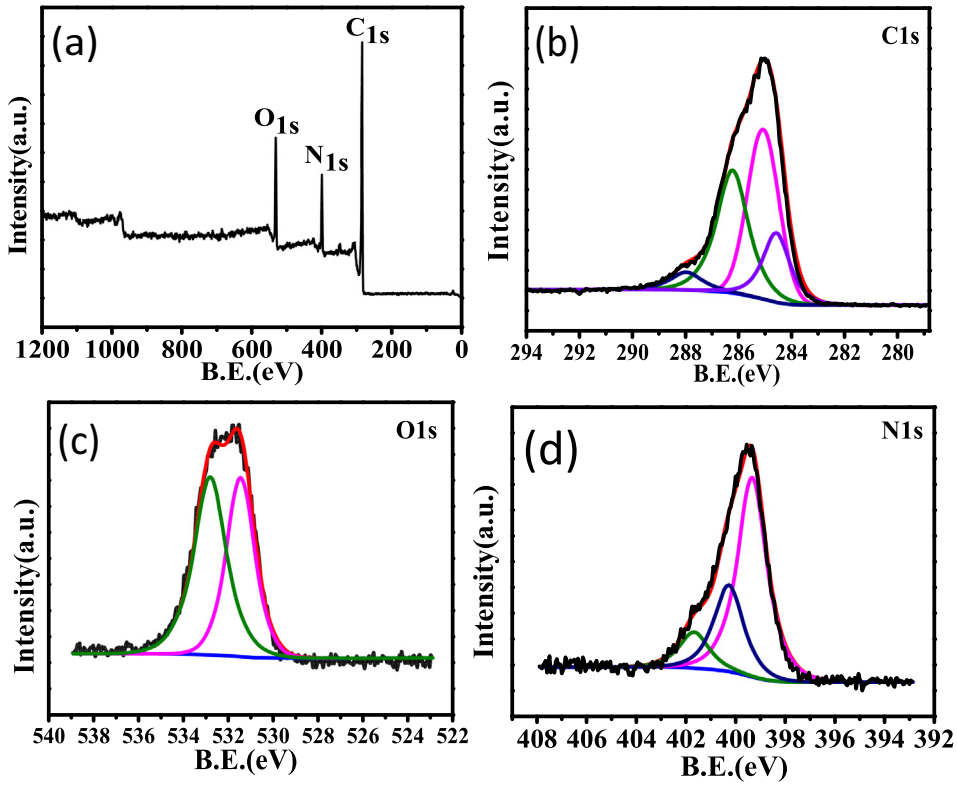

Fig. 5. (a) Is XPS scanning spectrum of N-doped CDs. XPS high resolution survey scan of (b) C1s, (c) N1s and (d) O1s region of N-GQDs.

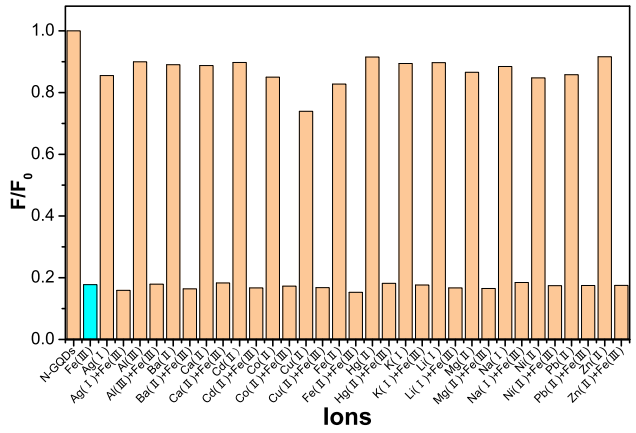

Fig. 6. Quenching effect of different metal ions on the intensity of N-GQDs PL (the concentration of all metal ions is 667 μM and the concentration of N-GQDs is 7.4 μg/mL).

3. Results and Discussion

3.1. Characterization of Nitrogen-doped Graphene Quantum Dots

The structures of marigold powder, GQDs and N-GQDs were characterized via FT-IR, as the Fig. 2(a) shows. In both peaks observed at 1613 cm^{-1} and 3437 cm^{-1} for marigold powder arose from C═C and C-OH groups of lutein Compared with the marigold powder. The bands of C═C, C—OH, C—O (1066 cm^{-1}), C—H (1420 cm^{-1}), H—C—H (2819 cm^{-1} and2942 cm^{-1}) and C═O (1729 cm^{-1}) of GQDs dramatically increased for the reason of the marigold powder undergoing high temperature pyrolysis to form turbostratic carbon after annealing. Turbostratic carbon has a kind of graphite structure, and contains a large number of C═C. A large number of C—OH, C—O and C═O had been introduced after acidification, the layer spacing of GQDs was increased, it shows in Fig. 1. Compared to the FT-IR spectrum of GQDs, the peaks of C—O and C═O of N-GQDs were almost disappeared. This might be due to oxygen radicals were destroyed after intramolecular decarboxylation reaction. However, some new peaks appeared in N-GQDs. The peak at 712 cm^{-1} arose from C—N [36]. The corresponding peak showed further broadening into higher energy due to the suggested formation of N—H groups in the range of 3300–3400 cm^{-1} [32]. These results indicated the successful incorporation of nitrogen atoms into the GQDs by the present synthetic process. The optical properties of N-GQDs were studied by UV–vis absorption and Photoluminescence (PL) spectroscopy. The UV–vis absorption spectrum of N-GQDs was exhibited in Fig. 2(b). The strong absorption at 294 nm was due to π-π* transitions of aromatic domains and the peak observed at approximately 320 nm with a weak shoulder was due to the n-π* transition [24]. According to the overview reported by Timur and sun, so far, the luminescence principle of GQDs has been described in different ways [37,38]. We speculated that the origin of GQDs luminescence in this work may be caused by surface states and defects [39]. As illustrated in Fig. 2(b), due to the addition of ethylenediamine, the fluorescence color of N-GQDs changed from green to strong blue under irradiation with 365 nm ultraviolet light, which proves that the doping of heteroatoms can change the fluorescence performance of quantum dots. As shown in Fig. 2(c), with the excitation wavelength increased from 300 to 360 nm, fluorescence spectrum peaks of N-GQDs ranged from 410 to 430 nm, the PL peaks of N-GQDs shift to longer wavelengths and its intensity decreased gradually, which maximum emission peak corresponding to the excitation wavelength of 340 nm. The 20 nm rad-shift of PL emission was presumed to be a strong electron affinity from N-doped in N-GQDs [40]. But Cai et al. thought the excitation-dependent fluorescence behavior might be due to the optical selection of different size N-GQDs and the surface defects of N-GQDs [41].

Therefore, the mechanisms of this need to be further confirmed.

In order to study the appearance of N-GQDs, transmission electron microscope (TEM) was used for further observations. As shown in Fig. 3(a), the average size of the N-GQDs was 3.2 nm and had a uniformly distributed. Fig. 3(b) showed the HRTEM images of the N-GQDs which clearly revealed the good crystal lattice of N-GQDs with a lattice spacing of 0.21 nm.

[42]. Due to this lattice structure of N-GQDs, significant D band at 1369 cm^{-1} and G band at 1597 cm^{-1} were observed in the Raman spectrum (Fig. 4(a)). A large intensity ratio G to D was 1.08, and this result was consistent with the report of Zhu et al. [43]. Fig. 4(b) shows the 2θ values in XRD showed an N-GQDs interlayer spacing of 0.37 nm at 24 Å.

The surface groups had also been explored by XPS (Fig. 5(a)). The total XPS spectrum proved that N-GQDs contained C, N and O elements (Table S1) [40]. C1s contained four different states of carbon atoms: C═C (284.6), C—C (285.1), C—N (286.2) and C═O (288.0) Fig. 5(b). Simultaneously, Fig. 5(c) is the spectrum of O1s. There were two absorption peaks at 531.4 eV and 532.8 eV, representing the presence of C—OH and C—O—C bonds respectively. In addition, the N1s spectrum (Fig. 5 (d)) also contained three strong absorption peaks at 399.4 eV, 400.3 eV and 401.7 eV, representing the presence of C—N, N—(C3) and N—H bonds respectively [44]. Moreover, the XPS analysis further demonstrated that the resultant of N-GQDs was composed of 68.38% C, 17.41% N and 14.21% O atoms. These results confirmed that N atoms had been successfully imported into GQDs and were consistent with the corresponding FT-IR spectroscopic results.

3.2. Experimental Condition Exploration

The prepared N-GQDs solution was neutral. In order to detect the fluorescence performance of N-GQDs in solution, different pH solutions were prepared. HCl and NaOH were used to prepare with different pH values, and PBS was used to replace neutral solutions. Fig. S1 showed the fluorescence changes at different pH values. Due to the protonation effects, the N-GQDs we prepared showed pH-dependent clearly. While, the pH had little change in fluorescence intensity between 4 and 11, in addition, the fluorescence intensity was the strongest when pH was 7. Compared with the previous reports on carbon quantum dots, it had

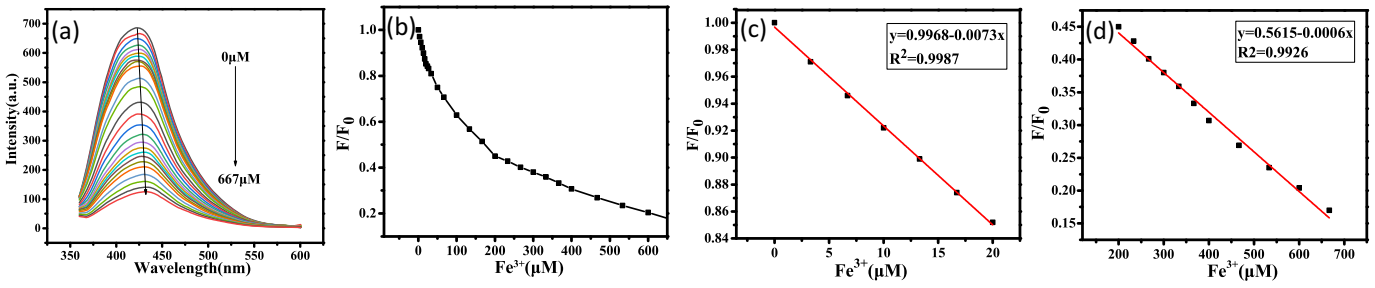

Fig. 7. (a) Is The quenching effect of Fe^{3+} with different concentration on N-GQDs PL, (b) is the point diagram of the quenching effect of different Fe^{3+} concentration on N-GQDs, (c) is the regression curve of Fe^{3+} (0–20 μM), (d) is the regression curve diagram of Fe^{3+} (200–667 μM).

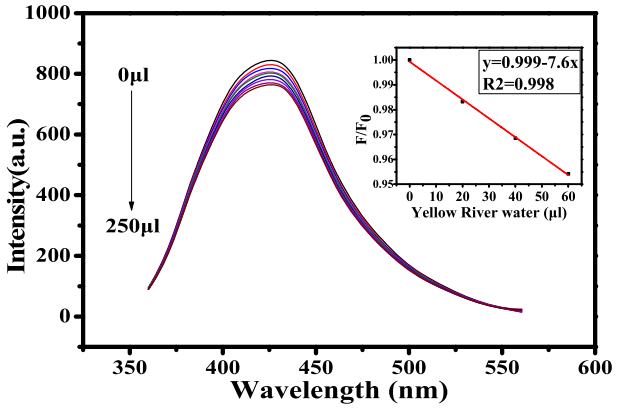

Fig. 8. The quenching effect of Fe^{3+} of Yellow River water with different volume on N-GQDs PL. The illustration is the quenching regression curve of the Yellow river water on N-GQDs.

better stability [45]. Therefore, it showed that the fluorescence performance of N-GQDs could be studied in a wide pH range. More importantly, the general environment was neutral and there was no need to adjust the pH of the actual solution. PBS was used as a buffer solution for fluorescence detection in subsequent experiments.

In order to explore whether N-GQDs had anti-light bleaching properties further, we put the N-GQDs under ultraviolet light for 30 min to record the change of the fluorescence intensity occurred every once in a while. We could see from the picture (Fig. S2), despite increasing exposure time, the fluorescence intensity of N-GQDs had hardly changed. It displayed a good stability and consistency with other reports about the preparation of carbon quantum dots [46].

3.3. Highly Selective and Competitive Detection of Fe^{3+} Ions with N-GQDs

In this work, N-GQDs were first used to detect metal ions in water medium because of the strong photoluminescence and specific surface functionalization through N-doped. The quenching effects of different positive ions including Ag^{+}, Al^{3+}, Ba^{2+}, Ca^{2+}, Cd^{2+}, Co^{2+}, Cu^{2+}, Fe^{2+}, Fe^{3+}, Hg^{2+}, K^{+}, Li^{+}, Mg^{2+}, Na^{+}, Ni^{2+}, Pb^{2+} and Zn^{2+} were studied. Interestingly, we found that when we added 200 μL of different ions to the cuvette, only Fe^{3+} had a significant quenching effect on fluorescence, whereas Cu^{2+} ions had a slight quenching effect. This might be a paramagnetic effect between Fe^{3+} and Cu^{2+}, which had also been reported in other reports [47–50]. Meanwhile, other ions showed little quenching of fluorescence of the N-GQDs (Please see Fig. 6). However, when we continued to add Fe^{3+} to other ion systems, the fluorescence intensity of those systems was quenched, which indicated that N-GQDs selectively detected Fe^{3+}. The quenching mechanism of Fe^{3+} on N-GQDs could be speculated that Fe^{3+} with the hydroxyl groups of N-GQDs have stronger affinity than other metal ions [43,51–53]. Fig. 7(a) showed the effect of different Fe^{3+} concentration on the fluorescence intensity of N-GQDs. The result showed that with the increasing of Fe^{3+} ions concentration the fluorescence intensity of N-GQDs decreased and the fluorescence peaks of N-GQDs-Fe (III) system had undergone red-shift from 422 to 433 nm, which suggested the formation of ground state compounds [54]. The results also showed that as the concentration of Fe^{3+} ions increased from 0 to 20 μM and from 200 to 667 μM, both the values of F/F_0 presented a good linear relationship (Fig. 7(b), (c) and (d)). The relative linear regression equation was expressed as $y = 0.9968–0.0073 \times (R^2 = 0.9987)$ and $y = 0.5615–0.0006 \times (R^2 = 0.9926)$. The K values are 7.3×10^3 L mol^{-1} and 0.6×10^3 L mol^{-1} respectively. Therefore, the limit of detections for Fe^{3+} was calculated to be 41.1 nM and 500 nM respectively based on $3\sigma/K$ (σ is the standard deviation of the N-GQDs for 10 times scans, K is the slope of the regression equation), which is compared with other works (Table S2) [55–58]. Therefore, there were both static and dynamic quenching processes in this fluorescence induction process [59]. And it shows a strong blue emission with 7.84% quantum yield (QY), this method was compared with other reports (Table S3) [60,61]. In addition, the quenching of Fe^{3+} to the fluorescence intensity of N-GQDs was completed within 1 min (Fig. S3).

In order to test the application of N-GQDs in real water quality, we investigated the fluorescence-sensing performance of N-GQDs on Fe^{3+} in Yellow River water from Lanzhou City, Gansu Province, China. The simple treatment of the water sample directly used for the quenching of fluorescence of N-GQDs was not adding other reagents. As shown in the illustration in Fig. 8, the F/F_0 of N-GQDs had a good linear relationship with the added water volume of the Yellow River when the amount of Yellow River water added was changed from 0 to 60 μL. Comparing the linear regression curve of the standard in Fig. 7(c), the same concentration of Fe^{3+} could be found, so the concentration of Yellow River water was 0.289 mM.

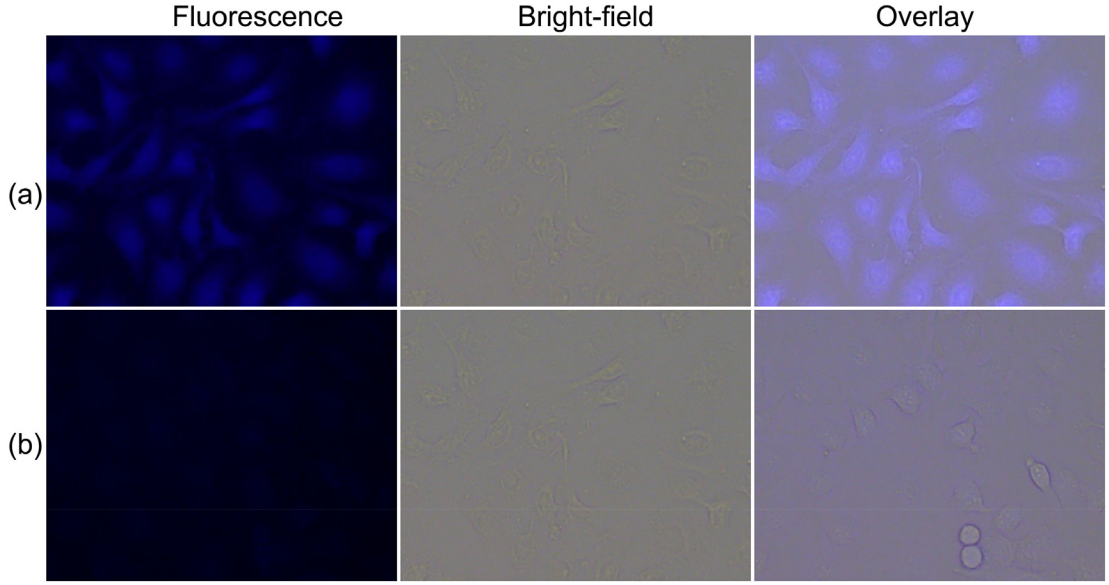

Fig. 9. Fluorescence images of HeLa cells. (a) is HeLa cells incubated with N-GQDs (200 μg/mL) for 6 h at 37 °C. (b) is Fe^{3+} (100 μM) were added into HeLa cells incubated for 1 h.

Fluorescence microscopy was used to observe the sensitivity of N-GQDs to Fe^{3+} in live HeLa cells. As Fig. 9(a) shown, HeLa cells were incubated with N-GQDs and showed blue fluorescence image. And the area showing blue fluorescence is in the cell, which indicated that N-GQDs can enter cells. The blue fluorescence of the cells almost disappeared after added Fe^{3+} (Fig. 9(b)). When the concentration of N-GQDs increased to 1000 μg/mL in Fig. S4, the cell viability reached 83%, and the concentration required for cell imaging was 200 μg/mL (the cell viability is 93%), which was much higher than the concentration required for cell imaging. However, the cell survival rate was only about 90% at the concentration of 12.5, which may be caused by the cells' inadaptability to the new living environment. Those demonstrated that N-GQDs have good biocompatibility and low toxicity, which can be used to detect Fe^{3+} in cells quickly and sensitively.

4. Conclusion

In summary, GQDs which contains a variety of functional groups could be prepared with a high-temperature pyrolysis method. Next, N-GQDs showed a strong blue fluorescence color with an average size of 3.2 nm were synthesized by hydrothermal method. The N-GQDs synthesized by this method have good stability, and the fluorescence intensity does not change significantly under wide pH range and ultraviolet lamp irradiation for a long time. When N-GQDs are used to detect various metal ions, only Fe^{3+} could be quenched the fluorescence of N-GQDs substantially. And there are two wide detection ranges and two low detection limits. There are both static and dynamic quenching processes in this fluorescence induction process. N-GQDs can be used to detect the concentration of Fe^{3+} in actual water and it has been applied to cell imaging successfully, which greatly improves the practical application value of N-GQDs.

Appendix A. Supplementary Data

Supplementary data to this article can be found online at https://doi.org/10.1016/j.saa.2019.03.044.

References

[1] J. Ju, W. Chen, Synthesis of highly fluorescent nitrogen-doped graphene quantum dots for sensitive, label-free detection of Fe (III) in aqueous media, Biosens. Bioelectron. 58 (2014) 219–225, https://doi.org/10.1016/j.bios.2014.02.061.

[2] Y. Fang, S. Guo, D. Li, C. Zhu, W. Ren, S. Dong, E. Wang, Easy synthesis and imaging applications of cross-linked green fluorescent hollow carbon nanoparticles, ACS Nano 6 (2012) 400–409, https://doi.org/10.1021/nn2046373.

[3] B. Kong, A. Zhu, C. Ding, X. Zhao, B. Li, Y. Tian, Carbon dot-based inorganic-organic nanosystem for two-photon imaging and biosensing of pH variation in living cells and tissues, Adv. Mater. 24 (2012) 5844–5848, https://doi.org/10.1002/adma.201202599.

[4] A. Krueger, Diamond nanoparticles: jewels for chemistry and physics, Adv. Mater. 20 (2008) 2445–2449, https://doi.org/10.1002/adma.200701856.

[5] K. Welsher, Z. Liu, S.P. Sherlock, J.T. Robinson, Z. Chen, D. Daranciang, H. Dai, A route to brightly fluorescent carbon nanotubes for near-infrared imaging in mice, Nat. Nanotechnol. 4 (2009) 773, https://doi.org/10.1038/nnano.2009.294.

[6] J. Jeong, M. Cho, Y.T. Lim, N.W. Song, B.H. Chung, Synthesis and characterization of a photoluminescent nanoparticle based on fullerene-silica hybridization, Angew. Chemie - Int. Ed. 48 (2009) 5296–5299, https://doi.org/10.1002/anie.200901750.

[7] K.P. Loh, Q. Bao, G. Eda, M. Chhowalla, Graphene oxide as a chemically tunable platform for optical applications, Nat. Chem. 2 (2010) 1015, https://doi.org/10.1038/nchem.907.

[8] X. Yan, X. Cui, L. Li, Synthesis of large, stable colloidal graphene quantum dots with tunable size, J. Am. Chem. Soc. 132 (2010) 5944–5945, https://doi.org/10.1021/ja1009376.

[9] N. Limchoowong, P. Sricharoen, Y. Areerob, P. Nuengmatcha, T. Sripakdee, S. Techawongstien, S. Chanthai, Preconcentration and trace determination of copper (II) in Thai food recipes using Fe_3O_4@Chi–GQDs nanocomposites as a new magnetic adsorbent, Food Chem. 230 (2017) 388–397, https://doi.org/10.1016/j.foodchem.2017.03.066.

[10] S. Li, Y. Li, J. Cao, J. Zhu, L. Fan, X. Li, Sulfur-doped graphene quantum dots as a novel fluorescent probe for highly selective and sensitive detection of Fe^{3+}, Anal. Chem. 86 (2014) 10201–10207, https://doi.org/10.1021/ac503183y.

[11] J. Deng, D. Lu, X. Zhang, G. Shi, T. Zhou, Highly sensitive GQDs-MnO_2 based assay with turn-on fluorescence for monitoring cerebrospinal acetylcholinesterase fluctuation: a biomarker for organophosphorus pesticides poisoning and management, Environ. Pollut. 224 (2017) 436–444, https://doi.org/10.1016/j.envpol.2017.02.024.

[12] X. Xu, R. Ray, Y. Gu, H.J. Ploehn, L. Gearheart, K. Raker, W.A. Scrivens, Electrophoretic analysis and purification of fluorescent single-walled carbon nanotube fragments, J. Am. Chem. Soc. 126 (2004) 12736–12737, https://doi.org/10.1021/ja040082h.

[13] J. Zhou, C. Booker, R. Li, X. Zhou, T.-K. Sham, X. Sun, Z. Ding, An electrochemical avenue to blue luminescent nanocrystals from multiwalled carbon nanotubes (MWCNTs), J. Am. Chem. Soc. 129 (2007) 744–745, https://doi.org/10.1021/ja0669070.

[14] R. Tabaraki, A. Nateghi, Nitrogen-doped graphene quantum dots: "turn-off" fluorescent probe for detection of Ag^{+} ions, J. Fluoresc. 26 (2016) 297–305, https://doi.org/10.1007/s10895-015-1714-y.

[15] M. Biswal, A. Banerjee, M.S. Deo, S. Ogale, From dead leaves to high energy density supercapacitor, Energy Environ. Sci. (2013) 84–121, https://doi.org/10.1039/b000000x.

[16] T. Zheng, J. Dahn, Effect of turbostratic disorder on the staging phase diagram of lithium-intercalated graphitic carbon hosts, Phys. Rev. B - Condens. Matter Mater. Phys. 53 (1996) 3061–3071, https://doi.org/10.1103/PhysRevB.53.3061.

[17] M. Bloor, H. Sampson, S. Baker, D. Walters, K. Dahlgren, E. Wadsworth, P. James, Room for manoeuvre? Regulatory compliance in the global shipping industry, Soc. Leg. Stud. 22 (2013) 171–189, https://doi.org/10.1177/0964663912467814.

[18] A. Wisitsoraat, J.P. Mensing, C. Karuwan, C. Sriprachuabwong, K. Jaruwongrungsee, D. Phokharatkul, T.M. Daniels, C. Liewhiran, A. Tuantranont, Printed organo-functionalized graphene for biosensing applications, Biosens. Bioelectron. 87 (2017) 7–17, https://doi.org/10.1016/j.bios.2016.07.116.

[19] H. Zhao, Y. Chang, M. Liu, S. Gao, H. Yu, X. Quan, A universal immunosensing strategy based on regulation of the interaction between graphene and graphene quantum dots, Chem. Commun. 49 (2013) 234–236, https://doi.org/10.1039/c2cc35503e.

[20] A. Ananthanarayanan, X. Wang, P. Routh, B. Sana, S. Lim, D.H. Kim, K.H. Lim, J. Li, P. Chen, Facile synthesis of graphene quantum dots from 3D graphene and their application for Fe^{3+} sensing, Adv. Funct. Mater. 24 (2014) 3021–3026, https://doi.org/10.1002/adfm.201303441.

[21] J. Annie Ho, H.-C. Chang, W.-T. Su, DOPA-mediated reduction allows the facile synthesis of fluorescent gold nanoclusters for use as sensing probes for ferric ions, Anal. Chem. 84 (2012) 3246–3253, https://doi.org/10.1021/ac203362g.

[22] G. He, M. Xu, M. Shu, X. Li, Z. Yang, L. Zhang, Y. Su, N. Hu, Y. Zhang, Rapid solid-phase microwave synthesis of highly photoluminescent nitrogen-doped carbon dots for Fe^{3+} detection and cellular bioimaging, Nanotechnology. 27 (2016) 395706, https://doi.org/10.1088/0957-4484/27/39/395706.

[23] L. Li, G. Wu, T. Hong, Z. Yin, D. Sun, E.S. Abdel-Halim, J.-J. Zhu, Graphene quantum dots as fluorescence probes for turn-off sensing of melamine in the presence of Hg^{2+}, ACS Appl. Mater. Interfaces 6 (2014) 2858–2864, https://doi.org/10.1021/am405305r.

[24] N. Yu, H. Peng, H. Xiong, X. Wu, X. Wang, Y. Li, L. Chen, Graphene quantum dots combined with copper(II) ions as a fluorescent probe for turn-on detection of sulfide ions, Microchim. Acta 182 (2015) 2139–2146, https://doi.org/10.1007/s00604-015-1548-y.

[25] F. Jiang, D. Chen, R. Li, Y. Wang, G. Zhang, S. Li, J. Zheng, N. Huang, Y. Gu, C. Wang, C. Shu, Eco-friendly synthesis of size-controllable amine-functionalized graphene quantum dots with antimycoplasma properties, Nanoscale. 5 (2013) 1137–1142, https://doi.org/10.1039/C2NR33191H.

[26] Y. Yin, Q. Liu, D. Jiang, X. Du, J. Qian, H. Mao, K. Wang, Atmospheric pressure synthesis of nitrogen doped graphene quantum dots for fabrication of BiOBr nanohybrids with enhanced visible-light photoactivity and photostability, Carbon N. Y. 96 (2016) 1157–1165, https://doi.org/10.1016/j.carbon.2015.10.068.

[27] S.-A. Wohlgemuth, R.J. White, M.-G. Willinger, M.-M. Titirici, M. Antonietti, A one-pot hydrothermal synthesis of sulfur and nitrogen doped carbon aerogels with enhanced electrocatalytic activity in the oxygen reduction reaction, Green Chem. 14 (2012) 1515–1523, https://doi.org/10.1039/C2GC35309A.

[28] Q. Li, S. Zhang, L. Dai, L. Li, Nitrogen-doped colloidal graphene quantum dots and their size-dependent electrocatalytic activity for the oxygen reduction reaction, J. Am. Chem. Soc. 134 (2012) 18932–18935, https://doi.org/10.1021/ja309270h.

[29] L. Yang, A. Qin, S. Chen, L. Liao, J. Qin, K. Zhang, Manganese(II) enhanced fluorescent nitrogen-doped graphene quantum dots: a facile and efficient synthesis and their applications for bioimaging and detection of Hg^{2+} ions, RSC Adv. 8 (2018) 5902–5911, https://doi.org/10.1039/C7RA12133D.

[30] L. Li, G. Wu, G. Yang, J. Peng, J. Zhao, J.-J. Zhu, Focusing on luminescent graphene quantum dots: current status and future perspectives, Nanoscale. 5 (2013) 4015–4039, https://doi.org/10.1039/C3NR33849E.

[31] Y. Li, Y. Zhao, H. Cheng, Y. Hu, G. Shi, L. Dai, L. Qu, Nitrogen-doped graphene quantum dots with oxygen-rich functional groups, J. Am. Chem. Soc. 134 (2012) 15–18, https://doi.org/10.1021/ja206030c.

[32] A. Suryawanshi, M. Biswal, D. Mhamane, R. Gokhale, S. Patil, D. Guin, S. Ogale, Large scale synthesis of graphene quantum dots (GQDs) from waste biomass and their use as an efficient and selective photoluminescence on–off–on probe for Ag^{+} ions, Nanoscale. 6 (2014) 11664–11670, https://doi.org/10.1039/C4NR02494J.

[33] Q. Hu, J. Chang, L. Tao, G. Yan, M. Xie, Z. Wang, Endoplasmic reticulum mediated necrosis-like apoptosis of HeLa cells induced by Ca^{2+} oscillation, J. Biochem. Mol. Biol. 38 (2005) 709–716http://www.ncbi.nlm.nih.gov/pubmed/16336787.

[34] T. Van Tam, N.B. Trung, H.R. Kim, J.S. Chung, W.M. Choi, One-pot synthesis of N-doped graphene quantum dots as a fluorescent sensing platform for Fe^{3+} ions detection, Sensors Actuators B Chem. 202 (2014) 568–573, https://doi.org/10.1016/j.snb.2014.05.045.

[35] Z. Li, L. Cao, P. Qin, X. Liu, Z. Chen, L. Wang, D. Pan, M. Wu, Nitrogen and oxygen co-doped graphene quantum dots with high capacitance performance for micro-

supercapacitors, Carbon N. Y. 139 (2018) 67–75, https://doi.org/10.1016/j.carbon.2018.06.042.
[36] L. Wang, W. Li, B. Wu, Z. Li, D. Pan, M. Wu, Room-temperature synthesis of graphene quantum dots via electron-beam irradiation and their application in cell imaging, Chem. Eng. J. 309 (2017) 374–380, https://doi.org/10.1016/j.cej.2016.10.022.
[37] T. Sh, Doped Carbon Dots for Sensing and Bioimaging Applications: A Minireview (2018)https://doi.org/10.3390/nano8050342.
[38] X. Sun, Y. Lei, Trends in analytical chemistry, Trends Anal. Chem. 89 (2017) 163–180, https://doi.org/10.1016/j.trac.2017.02.001.
[39] S.-L. Hu, K.-Y. Niu, J. Sun, J. Yang, N.-Q. Zhao, X.-W. Du, One-step synthesis of fluorescent carbon nanoparticles by laser irradiation, J. Mater. Chem. 19 (2009) 484–488, https://doi.org/10.1039/B812943F.
[40] S. Liu, J. Tian, L. Wang, Y. Zhang, X. Qin, Y. Luo, A.M. Asiri, A.O. Al-Youbi, X. Sun, Hydrothermal treatment of grass: a low-cost, green route to nitrogen-doped, carbon-rich, photoluminescent polymer nanodots as an effective fluorescent sensing platform for label-free detection of Cu(II) ions, Adv. Mater. 24 (2012) 2037–2041, https://doi.org/10.1002/adma.201200164.
[41] F. Cai, X. Liu, S. Liu, H. Liu, Y. Huang, A simple one-pot synthesis of highly fluorescent nitrogen-doped graphene quantum dots for the detection of Cr(VI) in aqueous media, RSC Adv. 4 (2014) 52016–52022, https://doi.org/10.1039/C4RA09320H.
[42] L.L. Li, J. Ji, R. Fei, C.Z. Wang, Q. Lu, J.R. Zhang, L.P. Jiang, J.J. Zhu, A facile microwave avenue to electrochemiluminescent two-color graphene quantum dots, Adv. Funct. Mater. 22 (2012) 2971–2979, https://doi.org/10.1002/adfm.201200166.
[43] S. Zhu, Q. Meng, L. Wang, J. Zhang, Y. Song, H. Jin, K. Zhang, H. Sun, H. Wang, B. Yang, Highly Photoluminescent Carbon Dots for Multicolor Patterning, Sensors, and Bioimaging ** Angewandte, (2013) 3953–3957. doi:https://doi.org/10.1002/anie.201300519.
[44] R. Liu, D. Wu, S. Liu, K. Koynov, W. Knoll, Q. Li, An aqueous route to multicolor photoluminescent carbon dots using silica spheres as carriers 13, Angew. Chemie. 121 (2009) 4668–4671, https://doi.org/10.1002/ange.200900652.
[45] D. Wu, X. Huang, X. Deng, K. Wang, Q. Liu, Preparation of photoluminescent carbon nanodots by traditional Chinese medicine and application as a probe for Hg^{2+}, Anal. Methods 5 (2013) 3023–3027, https://doi.org/10.1039/C3AY40337H.
[46] H. Huang, J.-J. Lv, D.-L. Zhou, N. Bao, Y. Xu, A.-J. Wang, J.-J. Feng, One-pot green synthesis of nitrogen-doped carbon nanoparticles as fluorescent probes for mercury ions, RSC Adv. 3 (2013) 21691–21696, https://doi.org/10.1039/C3RA43452D.
[47] H.-Y. Lin, P.-Y. Cheng, C.-F. Wan, A.-T. Wu, A turn-on and reversible fluorescence sensor for zinc ion, Analyst. 137 (2012) 4415–4417, https://doi.org/10.1039/C2AN35752F.
[48] A. Misra, M. Shahid, P. Srivastava, Optoelectronic behavior of bischromophoric dyads exhibiting Zn^{2+}/F-ions induced "turn-On/Off" fluorescence, Sensors Actuators B Chem. 169 (2012) 327–340, https://doi.org/10.1016/j.snb.2012.05.006.
[49] L. Xue, C. Liu, H. Jiang, Highly sensitive and selective fluorescent sensor for distinguishing cadmium from zinc ions in aqueous media, Org. Lett. 11 (2009) 1655–1658, https://doi.org/10.1021/ol900315r.
[50] Y.S. Yang, S.S. Ma, Y.P. Zhang, J.X. Ru, X.Y. Liu, H.C. Guo, A novel biphenyl-derived salicylhydrazone Schiff base fluorescent probes for identification of Cu^{2+} and application in living cells, Spectrochim. Acta - Part A Mol. Biomol. Spectrosc. 199 (2018) 202–208, https://doi.org/10.1016/j.saa.2018.03.060.
[51] R. V. Nair, R.T. Thomas, V. Sankar, H. Muhammad, M. Dong, S. Pillai, Rapid, Acid-Free Synthesis of High-Quality Graphene Quantum Dots for Aggregation Induced Sensing of Metal Ions and Bioimaging, (2017) 8051–8061. doi:https://doi.org/10.1021/acsomega.7b01262.
[52] F. Wang, Z. Gu, W. Lei, W. Wang, X. Xia, Q. Hao, Graphene quantum dots as a fluorescent sensing platform for highly efficient detection of copper(II) ions, Sensors Actuators B Chem. 190 (2014) 516–522, https://doi.org/10.1016/j.snb.2013.09.009.
[53] Y. Song, S. Zhu, S. Xiang, X. Zhao, J. Zhang, H. Zhang, Y. Fu, B. Yang, Investigation into the fluorescence quenching behaviors and applications of carbon dots, Nanoscale. 6 (2014) 4676–4682, https://doi.org/10.1039/C4NR00029C.
[54] S. Huang, H. Qiu, F. Zhu, S. Lu, Q. Xiao, Graphene quantum dots as on-off-on fluorescent probes for chromium(VI) and ascorbic acid, Microchim. Acta 182 (2015) 1723–1731, https://doi.org/10.1007/s00604-015-1508-6.
[55] T. Xu, J. Yang, J. Song, J. Chen, H. Niu, C. Mao, S. Zhang, Y. Shen, Sensors and actuators B: chemical synthesis of high fluorescence graphene quantum dots and their selective detection for Fe^{3+} in aqueous solution, Sensors Actuators B Chem. 243 (2017) 863–872, https://doi.org/10.1016/j.snb.2016.12.048.
[56] M. Shamsipur, K. Molaei, F. Molaabasi, M. Alipour, Talanta facile preparation and characterization of new green emitting carbon dots for sensitive and selective off/on detection of Fe^{3+} ion and ascorbic acid in water and urine samples and intracellular imaging in living cells, Talanta. 183 (2018) 122–130, https://doi.org/10.1016/j.talanta.2018.02.042.
[57] X. Gao, X. Zhou, Y. Ma, T. Qian, C. Wang, F. Chu, Applied surface science facile and cost-effective preparation of carbon quantum dots for Fe^{3+} ion and ascorbic acid detection in living cells based on the " on-off-on" fluorescence principle, Appl. Surf. Sci. 469 (2019) 911–916, https://doi.org/10.1016/j.apsusc.2018.11.095.
[58] Y. Guo, F. Cao, Y. Li, Sensors and actuators B: chemical solid phase synthesis of nitrogen and phosphor co-doped carbon quantum dots for sensing Fe^{3+} and the enhanced photocatalytic degradation of dyes, Sensors Actuators B Chem. 255 (2018) 1105–1111, https://doi.org/10.1016/j.snb.2017.08.104.
[59] T. Lai, E. Zheng, L. Chen, X. Wang, L. Kong, C. You, Y. Ruan, X. Weng, Hybrid carbon source for producing nitrogen-doped polymer nanodots: one-pot hydrothermal synthesis, fluorescence enhancement and highly selective detection of Fe(III), Nanoscale. 5 (2013) 8015–8021, https://doi.org/10.1039/C3NR02014B.
[60] J. Li, J. Song, X. Liang, Q. Ma, L. Shen, Y. Guo, F. Feng, A highly selective and sensitive fluorescence sensor for the detection of apigenin based on nitrogen doped carbon dots and its application in cell imaging, Anal. Methods 9 (2017) 6379–6385, https://doi.org/10.1039/c7ay02202f.
[61] Y. Dong, C. Chen, X. Zheng, L. Gao, Z. Cui, H. Yang, C. Guo, Y. Chi, C.M. Li, One-step and high yield simultaneous preparation of single- and multi-layer graphene quantum dots from CX-72 carbon black, J. Mater. Chem. 22 (2012) 8764–8766, https://doi.org/10.1039/C2JM30658A.